

Computational study of urban heat island of Putrajaya, Malaysia

Kenobi Isima Morris^{a,*}, Siti Aekbal Salleh^b, Andy Chan^a, Maggie Chel Gee Ooi^a, Yousif Abdalla Abakr^a, Muhammad Yaasiin Oozeer^a, Michael Duda^c

^a Faculty of Engineering, University of Nottingham Malaysia Campus, Selangor, Malaysia

^b Faculty of Architecture Planning and Surveying, Universiti Teknologi MARA, Selangor, Malaysia

^c National Center for Atmospheric Research NCAR Boulder, CO, USA



ARTICLE INFO

Article history:

Available online 8 May 2015

Keywords:

Garden-city concept
Urban heat island
Local climate zone

ABSTRACT

The administrative capital of Malaysia, Putrajaya, is one of those cities built on the garden-city concept, however, few studies have been devoted to confirm the validity of the concept. Numerical mesoscale Weather Research and Forecasting (WRF) Model was coupled with Noah land surface model and a single layer urban canopy model (UCM) to investigate the existence and distribution of UHI, and the behaviour of urban canopy layer (2-m) temperature of Putrajaya city. Suitability of the model WRF employed in studying UHI phenomenon in the tropical city of Putrajaya, Malaysia was determined. Precincts in Putrajaya city were classified into local climate zones (LCZs) and the contribution of urban fabrics on the spatial and temporal variations of UHI was also investigated. Results of the model were verified with in situ studies of the area, and observational data from Alam Sekitar Malaysia Sdn Bhd (ASMA). Comparison with ASMA observational and in situ data reveals a satisfactory performance of the model. UHI intensity of Putrajaya exhibits a diurnal profile; increasing during the night to a peak value and then diminishing in the morning with a negligible value during mid-day. During the night hours, the UHII ranges from 1.9 °C to 3.1 °C in some of the precincts (LCZs) considered. Overall, average daily intensity of 0.79 °C heating was noted in Putrajaya for the study duration. The overall effect of urbanized LCZs heating of Putrajaya was normalized by the total amount of area reserved for vegetation.

© 2015 Elsevier Ltd. All rights reserved.

1. Introduction

Putrajaya is a planned model concept city and administrative capital of Malaysia. Being first of its kind in the region, it is built to reflect the country's commitment to green environment and to accommodate the growing size of the Malaysian federal government ministries and national level civil servants. It is structured to accommodate all diplomatic activities for the country and to showcase the nation's modernization agenda (Moser, 2010). Putrajaya is located in Klang Valley, 25 km south of Kuala Lumpur on coordinates 2°55'00" N 101°40'00" E and covers an approximate area of 49 km² (Fig. 1a) which was previously covered by green vegetation, rubber and oil palm plantation prior to its development.

Unlike other cities sprawling from a core with a clear chronology of expansion over decades (Alsharif & Pradhan, 2013; Inostroza, Baur, & Csaplovics, 2013; Martilli, 2014; Zeng, Liu, Stein, & Jiao,

2015), Putrajaya follows the concept by Sir Ebenezer Howard in the United Kingdom (Howard, 1946); where cities are planned and built on undeveloped land with a planning garden-city concept (Bigon, 2012). Several cities such as Maringa in Brazil (Macedo, 2011), French Dakar in Senegal (Bigon, 2012) and Putrajaya (Chin, 2006) have been built with this concept, most of which were politically envisioned (Moser, 2010). Despite the lush and colourful canopy afforded to the cities with planned urbanization, most have failed to integrate local climate conditions into the garden-city concept, leading to negative consequences such as poor environmental and ecological conditions (Johnson, 2008; Xin, Bo, & Li, 2011). Building cities that are responsive to the local climate conditions and contribute sustainable environment are some of the challenges facing urban planners.

Urban heat island is a common phenomenon in cities (Hien & Jusuf, 2010). The urban-rural temperature difference – urban heat island intensity (UHII) is the most cited measure of climatic modification of a city in environmental science (Stewart & Oke, 2012). UHI is a consequence of urbanization. Urbanization induces significant changes in the properties of land surface which, in turn, modifies the surface energy balance (SEB) of urban areas (Stewart & Oke, 2012) thereby influencing energy consumption

* Corresponding author at: Department of Mechanical, Materials and Manufacturing Engineering, University of Nottingham Malaysia Campus, 43500 Jalan Broga, Semenyih, Selangor, Malaysia. Tel.: +60 126837465.

E-mail address: kenobimorris@yahoo.com (K.I. Morris).

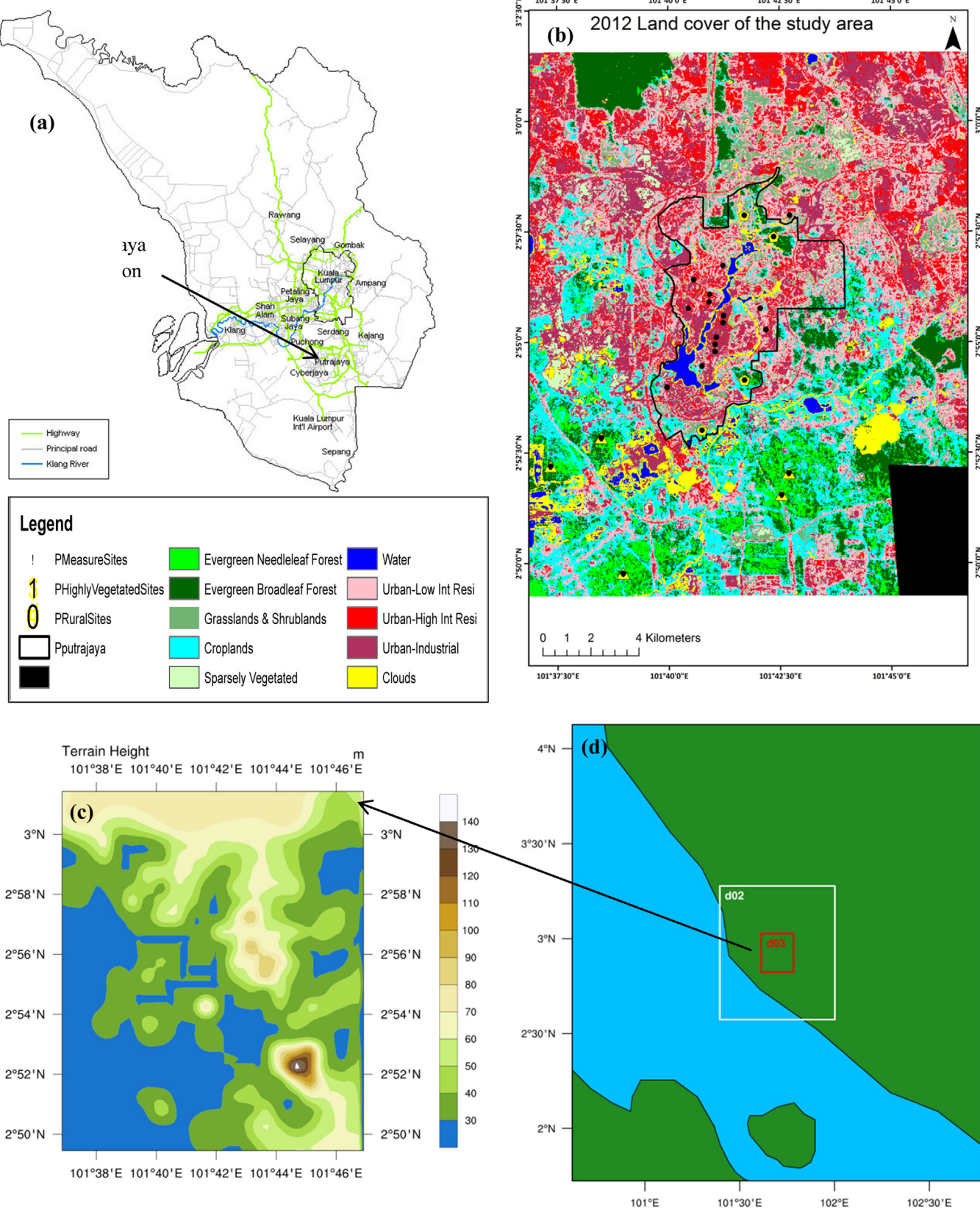


Fig. 1. (a) Putrajaya location. (b) Putrajaya 2012 Land use and land cover. (c) Terrain height (m) of the inner domain (relative to mean sea level). (d) 3 one-way nested domain configuration for WRF simulation.

(Akbari, 2005; Hirano & Fujita, 2012; Kolokotroni, Giannitsaris, & Watkins, 2006; Konopacki & Akbari, 2002; Martilli, 2014), air quality (Rosenfeld, Akbari, Romm, & Pomerantz, 1998; Wang et al., 2012), heat related discomfort, high mortality rate (Enete, Officha, & Ogbonna, 2012; Fire and Disaster Management Agency of Japan, 2011; Ihara, Kusaka, Hara, Matsuhashi, & Yoshida, 2011; Md Din et al., 2014; Uejio et al., 2011) and local and regional atmospheric circulations (Feng, Wang, Ma, & Liu, 2012; Marrapu, 2012; Miao et al., 2009). UHIs do not have a direct influence on global temperatures (IPCC, 2001); however, they do have impact on local temperatures used to assess climate changes (Barker, 2007; Van Weverberg, De Ridder, & Van Rompaey, 2008).

Contrast in SEB in urban and rural areas as a consequence of the imbalance in the amount of heat energy stored during the day is the primary cause of UHI development (Oke, 1982). The Earth's natural vegetation with a near-uniform surface roughness and evapotranspiration properties are being replaced with urban fabrics (such as asphalts, concretes, bricks and metals) characterized with high thermal properties (Rosenfeld et al., 1998; Taha, 1997; Yang, 2013). The surface modifications caused by canyon-like geometry and altered thermal properties of natural vegetation enable built-up areas to store more radiated heat during the day than rural areas. Following sunset, urban and rural temperatures begin to diverge thereby generating the heat island in the canopy-layer of the built up areas. As a result of the open exposure and unobstructed clear sky view factor of rural areas, cooling starts quickly after sunset, unlike built up areas with slow cooling rate. This is attributed to reduced sky view factor and re-radiation of the stored heat energy during the day (Offerle, Grimmond, & Fortuniak, 2005; Taha, 1997). The heat island stays in the canopy-layer overnight, until sunrise when daily solar radiation cycle begins and rural areas start warming up (Giannaros, Melas, Daglis, Keramitsoglou, & Kourtidis, 2013).

Outdoor thermal conditions in urban areas are of major concern in the tropical region of Southeast Asia (SEA). In temperate climates, the maximum UHI effect could be noticed only during summer seasons and could be beneficial at times (Oke, 1988a, 1988b). However, due to close proximity of the tropical regions to the equator and high exposure of the region to solar radiation, UHI effect is felt during hot dry season and every other time of the year (Tran, Uchihama, Ochi, & Yasuoka, 2006). Inadequate shading and green spaces are unable to intercept and balance the heat from direct solar gains. Also conventional use of dark materials in buildings and pavements trap more of the sun's energy during the day and re-radiates it at night. This has led to air and surface temperature increases with consequent influence on human thermal comfort and energy consumption in the tropics (Enete et al., 2012; Shaharuddin, Noorazuan, Yaacob, & Noraziah, 2011; Wijeyesekera et al., 2012).

Though, there are few studies on Klang Valley (which encompasses Putrajaya area, Kuala Lumpur and Selangor) on the subject of UHI, most are in situ studies (Ahmad, Hashim, & Jani, 2009; Ahmad, Hashim, Jani, Aiyub, & Mahmod, 2010; Elsayed, 2011, 2012, 2012b; Ibrahim & Samah, 2011; Sani, 1984; Yusof & Johari, 2012; Yusuf, Pradhan, & Idrees, 2014) and little or no attention have been given to the subject numerically, especially for prognostic studies. Putrajaya, a city with its emergence from an undeveloped palm plantation or almost green vegetation (Moser, 2010) fits to be studied, to understand the effectiveness of the "garden-city concept" adopted during its design and planning. Due to insufficient data in the area, this study has been validated with an hourly surface observational data from Alam Sekitar Malaysia Sdn Bhd (ASMA) and corroborated with a recently published in situ study by Ahmed et al. (2014). To bridge the gap in the study of UHI in the region, the study aims to investigate the temporal and spatial variation of the UHI of Putrajaya, canopy layer (2-m) air temperature, influence of surface materials and classification of Putrajaya city into

different LCZs using the advanced core of the NCAR non-hydrostatic mesoscale model, WRF-ARW. This will evaluate the responsiveness of the garden-city concept to the surrounding environment and as well lay a roadmap for subsequent studies on the subject in the region.

2. Data sources

To understand the climatology of Putrajaya city, data from different sources were used in this research. Six hourly ($1.0^\circ \times 1.0^\circ$) global Final (FNL) Analysis data were used as Global Forecast System (GFS) data for initial and lateral boundary conditions for the simulations. These data were obtained from the National Centre for Environmental Prediction (NCEP) (NCEP, 2000). Hourly surface observational data from Alam Sekitar Malaysia Sdn Bhd (ASMA) (DOE, 2013) and Ahmed et al. (2014) were used to verify the canopy layer (C-L) air temperatures (2-m temperature) from the numerical calculations employed. Different digital satellites images were also used for depiction and identification of locations, land use (Fig. 1b) and local climate zone (LCZ) classification of the area, using Stewart & Oke (2012) guidelines.

2.1. Description of the study area

Putrajaya ($2^{\circ}55'00''$ N $101^{\circ}40'00''$ E) is located in the west peninsula of Malaysia and encompassed by the Klang Valley (Moser, 2010) (Fig. 1a). In line with the Putrajaya's master plan, the development of the city which started in 1993 is due to be completed by the year 2025 (Ahmed et al., 2014). The master plan is characterized by the "garden-city" concept, integrating physical features such as landforms, vegetation and water bodies to produce the green scenery of the city. Keeping with the country's pledge to adhere to environmental standards, about 38% of the total land area of Putrajaya is reserved for wetlands, green space and water body (Chin, 2006). However only about 60% of the intended master plan has been completed as of 2012 (Ahmed et al., 2014). According to the Malaysian Department of Statistics (DOS) Putrajaya is host to approximate 100,000 residents of the projected 350,000 residents when completed (Moser, 2010).

Situated few degrees off north of the equator and with an average elevation of 30 m (Fig. 1c) (Moser, 2010), Putrajaya sits on a hilly terrain with a humid and hot weather all year. Rainfall averages 2–3 m in a year and falls heavily during the monsoon season, depositing about 10–30 cm within few hours (Bunnell, 2002). Proximity to the equator exposes the area to high solar radiation accounting to about 6.1 h of sunshine per day all year round and hence the hot and humid climate experienced; with a near steady average air temperature (27.5°C and 25°C , maximum and minimum respectively), 62.6% humidity and wind speed in the range of 0–7.5 m/s (Shahidan, Jones, Gwilliam, & Salleh, 2012). The main boulevard measures 100 m wide, and extends 4.2 km from the northeast to the southwest of Putrajaya, and cut across five core precincts (1, 2, 3, 4 and 5) of the area (Fig. 2) (Shahidan et al., 2012). Surrounded by government symmetric buildings oriented northwest to southeast, the main boulevard separates the administrative area with the surrounding streets. The urban form of Putrajaya area could simply be described as a characteristic fusion of different climate zones (LCZs).

2.2. Meteorological data

In an attempt to investigate the urban heat island of the city, Ahmed et al. (2014) conducted an in situ measurement of surface temperature, ground temperature (LST) and wind velocity from 14 to 16th July, 2012 along the main boulevard covering precincts 1, 2, 3 and 4.

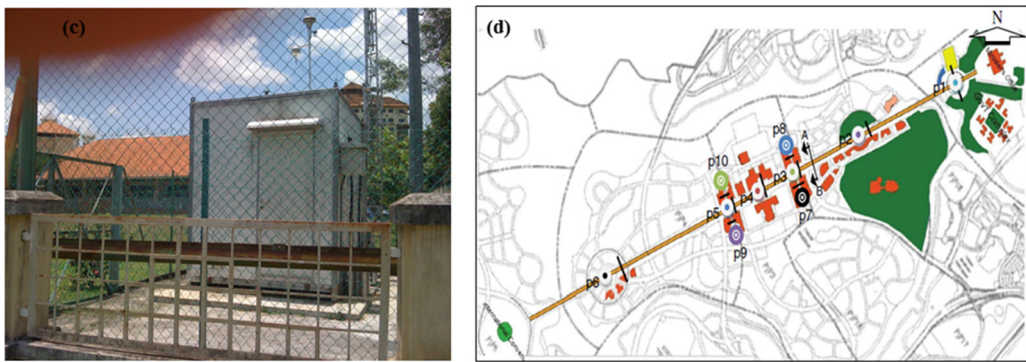


Fig. 2. CAQM station and Putrajaya main boulevard and intersecting precinct (Ahmed et al., 2014).

Data were also collected from ASMA, a private company in Malaysia saddled with maintenance and collation of hourly meteorological data using a network of 52 Continuous Automatic and Manual Air Quality Monitoring (CAQM) stations in Malaysia. For this study, station CAC053 ($02^{\circ}55'54.9\text{ N}$ – $101^{\circ}40'54.5\text{ E}$) is the designated ID of the only CAQMS station situated within Putrajaya. The station is fitted with sensor to measure air temperature at an altitude of 3 m. CAC053 is located in precinct 8 and in an open field with nearby classrooms and source area characterized by open low-rise LCZ built type.

3. Methodology and evaluation

Using established guidelines (Aguilar, Auer, Brunet, Peterson, & Wieringa, 2003; Oke, 2004; Stewart & Oke, 2012) for metadata collections and source area delineation (Stewart, Oke, & Krayenhoff, 2014), source areas were set to encompass a 100 m radius from sites of data collections in dense urban surroundings (e.g. city core) and 200 m radius for more open fetch areas (e.g. city outskirts). This is necessitated by varying magnitude of advection within dense and open fetch areas, and thus the impact on transport of re-radiated fluxes during calmed nights. Horizontal spatial classification of LCZ zone were adopted from the definition of 0.1–10 km (Oke, 1988a, 1988b; Stewart et al., 2014). Hence, the definitions of immediate land cover types and LCZ used in characterizing different sites in this study (Table 1).

3.1. Numerical configuration

To study the temperature distribution and UHI of the nascent Putrajaya city, 13th–28th July 2012 were simulated with interest on the 2-m air temperature. These days were selected to coincide with the dates studied by Ahmed et al. (2014) to establish the basis for comparison and validation of the model. Version 3.5 of the WRF-ARW (Advanced Research Weather) model was used as the meteorological model for numerical calculations (Skamarock et al., 2008). This system combines the Unified Noah land-surface model (LSM) (Chen & Dudhia, 2001), coupled with the single-layer urban canopy model (UCM).

Planetary boundary layer (PBL) was handled with the Yonsei University (YSU) scheme (Hong, Noh, & Dudhia, 2006), combined with the coupled Noah/UCM land surface model. It is considered to perform well in high resolution urban climate applications (Hong et al., 2006; Lin et al., 2008). Other physics parameterizations include a long-wave Rapid Radiative Transfer Model (RRTM) (Mlawer, Taubman, Brown, Iacono, & Clough, 1997), a short-wave radiation scheme based on Dudhia cloud radiation scheme (Dudhia, 1989) and a surface-layer scheme based on the Monin–Obukhov similarity theory. The WRF single-moment six-class (WSM-6) microphysics scheme was applied to all domains (Dudhia, Hong, &

Lim, 2008; Hong, Ji & Chen, 2004), while parameterization of cumulus convection was completed using Kain–Fritsch scheme (Kain, 2004).

Three one-way nested domains (Fig. 1d) was used with horizontal grid spatial resolutions of 2.7, 0.9 and 0.3 km with corresponding grid sizes of 90×100 , 76×88 and 64×76 , from West to East and South to North, for parent (d01), 1st nested (d02) and innermost (d03) domain respectively. WRF uses terrain-following hydrostatic-pressure vertical coordinate system proposed by (Laprise, 1992) to resolve the vertical layers of the model. In this study, 32 vertical levels were used, 18 of which were reserved in the lower 2 km of the model to further resolve the lower atmosphere, while the model top layer was specified at 100 hPa. This is to accommodate the frequent changes of atmospheric variables in the lower boundary layer and as well to effectively handle the small scale features near the Earth's surface. However, the coarse vertical spacing of the sigma higher levels was to reduce computational cost (Chou, 2011).

Updated high resolution 20-category MODIS data land use and land cover (LULC) classification of the International Geosphere–Biosphere Programme and modified for the Noah land surface model (NCAR, 2014), using remote sense data of the area, recent land cover classification and Google Earth images as reference for modification, were used for the land use and land cover of the study; with 2-arc-min, 30-arc-s, and 30-arc-s spatial resolution used for d01, d02 and d03 respectively (Skamarock et al., 2008). The need to understand phenomena such as urban heat island in microclimates has made the need for high resolution LULC classification more imperative.

Noah land surface model (LSM) was employed to parameterized the land surface processes (Chen & Dudhia, 2001). The updated Noah LSM is a land surface-hydrology model (Giannaros et al., 2013) which serves to provide surface sensible and latent heat fluxes, account for sub-grid fluxes and skin temperature as lower boundary conditions to the boundary layer scheme of the WRF. The model (Noah LSM) has a single-canopy layer with four soil layers of varying thicknesses (10, 30, 60 and 100 cm); 10 and 100 cm being the top and bottom layers respectively. This equates the total soil depth of the Noah LSM to 2 m, with the upper and lower 1 m of the soil serving as the root zone depth and reservoir with gravity drainage respectively (Giannaros et al., 2013).

Single-layer UCM has a unique simplified two-dimensional urban geometry model, considering building height, roof and road width and assuming street canyons of infinite length. It also includes solar trapping and reflection of radiation and shadowing effects, which is determined by the street canyon dimensions and orientation, as well as solar azimuth angle. Thus, energy and momentum transfer between urban environment and the atmosphere could be calculated by computing surface temperatures and heat fluxes of roof, wall and road within the considered area. In this

Table 1

Characteristics of data extraction sites during the study.

| Name | Latitude (°N) | Longitude (°E) | Altitude (m.a.s.l ^a) | Built type (LCZ) | Immediate land cover of sites source area |
|------|---------------|----------------|----------------------------------|------------------|---|
| P3 | 2°54'57.06" | 101°41'2.40" | 32 | Open midrise | Pave surface |
| P4 | 2°54'27.72" | 101°40'44.40" | 38 | Sparingly built | Low plants and paved surface |
| P6 | 2°53'58.85" | 101°39'57.60" | 25 | Sparingly built | Bare rock/soil |
| P7 | 2°55'45.88" | 101°40'26.40" | 42 | Open midrise | Paved surface |
| P8 | 2°56'5.10" | 101°40'55.20" | 42 | Compact low-rise | Paved surface |
| P9 | 2°56'24.86" | 101°40'33.60" | 39 | Open midrise | Paved surface |
| P10 | 2°56'44.09" | 101°41'13.20" | 32 | Open low-rise | Paved surface |
| P12 | 2°57'23.08" | 101°42'21.60" | 49 | Compact low-rise | Bare soil and dense trees |
| P13 | 2°57'52.16" | 101°41'42.00" | 35 | Sparingly built | Bare soil and dense trees |
| P17 | 2°55'16.79" | 101°42'10.80" | 43 | Open midrise | Scattered trees |
| P19 | 2°54'8.46" | 101°41'42" | 49 | Sparingly built | Low plants |
| P20 | 2°53'0.64" | 101°40'44.40" | 14 | Sparingly built | Low plants |
| BLV1 | 2°55'26.40" | 101°41'13.20" | 29 | Sparingly built | Paved surface |
| BLV2 | 2°54'47.45" | 101°41'2.40" | 37 | Sparingly built | Paved surface |
| IR | 2°57'52.16" | 101°42'43.20" | 49 | Sparingly built | Low plants |
| TMP | 2°55'45.88" | 101°42'3.60" | 47 | Open low-rise | Paved surface and scattered trees |
| Obs1 | 2°55'36.03" | 101°41'13.90" | 31 | Open midrise | Paved surface |
| Obs2 | 2°55'6.67" | 101°41'4.12" | 39 | Open midrise | Paved surface |
| Obs3 | 2°55'54.9" | 101°40'54.5" | 33 | Open low-rise | Open field and paved surface |
| R1 | 2°52'2.42" | 101°42'41.40" | 23 | Sparingly built | Dense trees |
| R2 | 2°52'50.52" | 101°38'28.68" | 19 | Sparingly built | Dense trees and low plants |
| R3 | 2°52'12.06 | 101°37'20.28" | 14 | Sparingly built | Dense trees |
| R4 | 2°49'46.30" | 101°38'57.84" | 12 | Sparingly built | Open field and Low plants |
| R5 | 2°51'33.09" | 101°42'31.68" | 44 | Sparingly built | Dense trees |

^a Above sea level.

study, the UCM model was modified to reflect the prevailing urban morphological and surface conditions of Putrajaya using information derived from (Aekbal, Abd, Mohd, & Wan, 2013; Ahmed et al., 2014; Shahidan et al., 2012; Stewart & Oke, 2012). Though, the single-layer urban canopy model (UCM) coupled with the WRF model is considered an effective tool in predicting urban heat island of urban areas (Subramania Pillai & Yoshie, 2012), it is yet to be validated in tropical region of Malaysia. This study used both in situ and meteorological observation to corroborate the performance of the WRF coupled to the Noah LSM and UCM.

3.2. Model initialization

1° × 1° spatial resolution and 6 h temporal resolution operational global atmospheric final re-analysis (FNL) surface and pressure level data of the NCEP were used for initialization of the model simulation. In the surface boundary layer and at some sigma layers (tropopause), the data are available on the surface at 26-mandatory and other pressure levels starting from 1000 mbars to 10 mbars. Parent domain (d01) lateral boundary conditions were linearly interpolated from the NCEP FNL 6-hourly data used, while lateral boundary conditions for d02 and d03 were supplied via interpolated from the parent domain. The 4-layers (10, 30, 60 and 100 cm) of the Noah LSM temperature and soil moisture values were also initialized from the NCEP-FNL data. For the numerical simulation, model run was initiated at 12:00 UTC of 12th July, 2012 (corresponding to 20:00 MST¹ of 12th July, 2012) for a total run duration of 390 h with the first 12 h used as spin-up time for the model.

3.3. Model evaluation

Series of simulations were conducted with the WRF model to obtain set of dynamics and physics options with reduced bias to acceptable range before proceeding with model set-up for the study. Air temperature is an important parameter in urban climatology and has been used in several published studies to validate

Table 2
Statistical summary of locations validated.

| Statistical tool | MBE (°C) | MAE (°C) | RMSE (°C) | R ² |
|------------------|----------|----------|-----------|----------------|
| Obs1 | -0.21 | 0.78 | 0.98 | 0.84 |
| Obs2 | -0.62 | 0.91 | 1.17 | 0.85 |
| Obs3 | 1.63 | 1.69 | 2.03 | 0.81 |

different model performances (Giannaros et al., 2013; Hu, Yu, Chen, Li, & Liu, 2012; Mercader, Codina, Sairouni, & Cunillera, 2010; Shem & Shepherd, 2009). To establish a common basis for comparison of model and observed results, model results were obtained at same locations and corresponding time as observations.

Four statistical tools were employed in this study to evaluate the performance of the model used for the predicted results (*P*) and observed results (*O*), both for ASMA and Ahmed et al. (2014) (P3 and P4) data. Mean bias error (MBE), mean absolute error (MAE), root mean square error (RMSE) and Pearson correlation coefficient (*R*) were used to access model performance and agreement with observed data. Comparison of the WRF simulated and observed results in each case indicate good correlation between *P* and *O* (Figs. 3(a, b) and 4 and Table 2). The model has overestimated the canopy layer air temperature for ASMA station CAC053, though, with MAE magnitude within acceptable range (Fig. 3 and Table 2). The model has performed relatively well when compared with in situ observation by Ahmed et al. (2014) as in Fig. 4.

4. Results and discussion

4.1. Canopy-layer air temperature

The intensity of solar radiation reaching a given location on the earth's surface depends on the angle (azimuth angle) sunlight strikes the earth's ground surface. Fig. 5 presents 24 h simulated C-L temperature profile average over the nineteen extraction sites (Table 1) for the duration of study. C-L temperature profile of the city exhibits same diurnal profile as observed in other cities (Middel et al., 2012; Qiao, Tian, & Xiao, 2013; Sailor & Lu, 2004). Mean maximum and minimum temperatures of 24.5 °C and 31.2 °C were respectively observed at 0800 and 1600 MST (Fig. 5).

¹ Malaysian Standard Time.

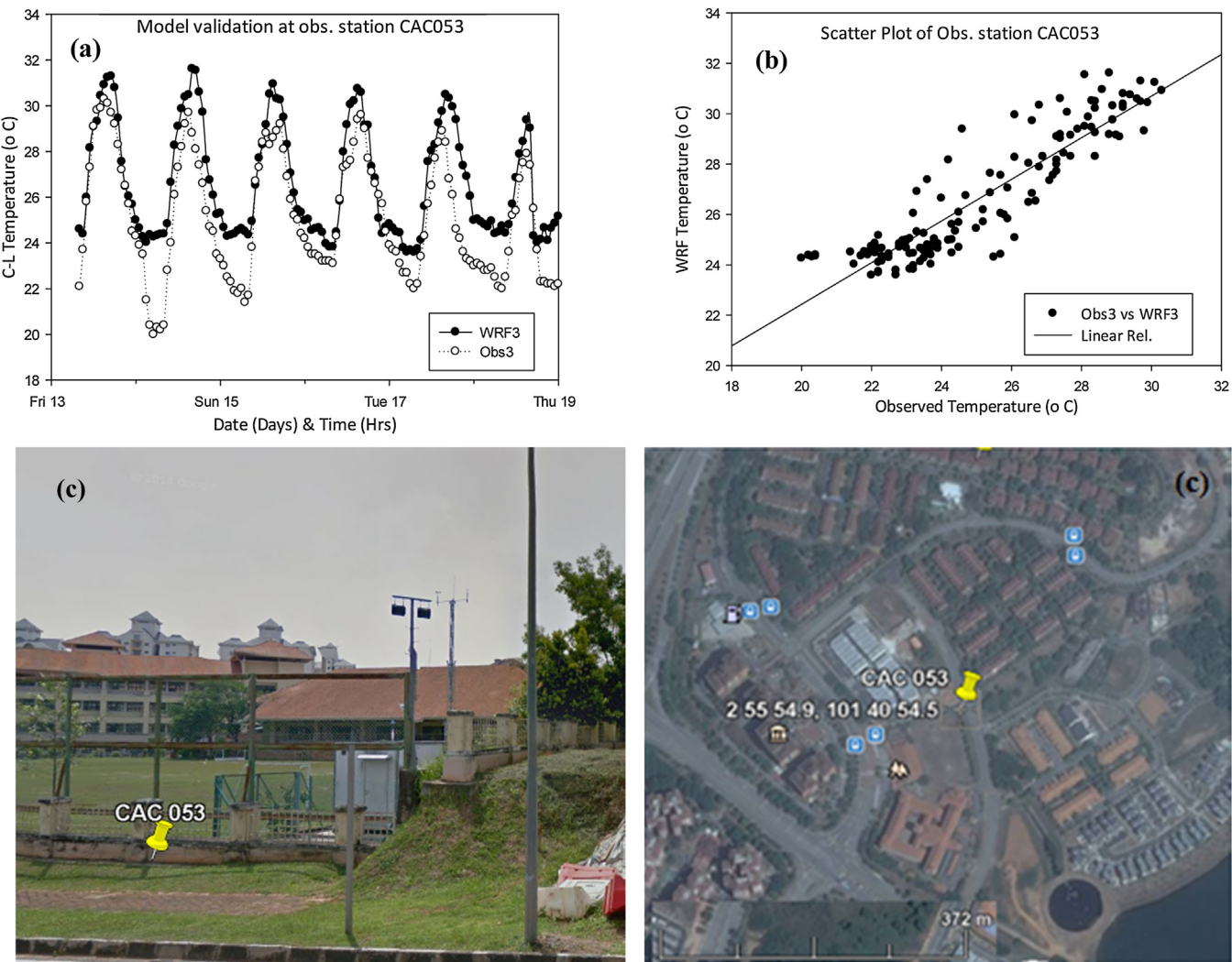


Fig. 3. (a) Model validation at Putrajaya ASMA station CAC053, (b) scatter plot for canopy layer air temperatures of observation station CAC053 and (c) location of ASMA station (Source: Google-Earth). WRF3 indicates model results and Obs3 for observed.

Fig. 6 shows the WRF canopy-layer (C-L) air temperatures for 13th of July, 2012 at different period characterized by temporal and spatial heating of the urban canopy. The model was able to capture the spatial and temporal variation of C-L air temperatures. Modelled spatial variation of C-L air temperature is due to the differential heating of different LCZs in the study area (Stewart & Oke, 2012). The LCZs (Table 1) are marked with different built and land cover types exhibiting different surface albedo resulting from the composition of the surface materials. Temporal C-L temperatures are driven by the diurnal cycle of sunrise and sunset.

4.2. Canopy-layer UHI

Urban C-L extends vertically from ground level up to the mean roof level of any given local urban climate zone; the urban-rural and LCZs (LCZ-LCZ) temperature contrast observed within this layer is referred to as the C-L UHI (Oke, 1982). As discussed in various literature (Giannaros et al., 2013; Stewart, 2011), caution was observed in sites selections process to eliminates unwanted effects that surface relief, elevation and other surface variability would impact on the magnitude of UHI. 24 sites with similar topographic features (Table 1) were selected for this study. Nineteen of which are within Putrajaya; representing different LCZs and Five (R1, R2, R3, R4 and R5) representing rural/semi-urban

conditions, situated few kilometres south of Putrajaya (Fig. 1b). Thus, induced influence of surrounding local climates due to advection and transport were minimized by locating the rural stations in areas isolated from other urban influence. To ensure UHII are correctly interpreted, 40 m (Table 1) maximum elevation difference between sites was used as criterion for sites selection (Giannaros et al., 2013).

Malaysia experienced differential precipitation between local climates and thus days (13th, 15th, 18th, 23rd, and 26th of July, 2012) with similar favourable synoptic conditions (such as calm days without precipitation, low surface wind speed and weak horizontal pressure gradient resulting in clear skies) for the study of UHI were considered to investigate the rural-urban C-L UHI experienced in Putrajaya. Precipitation data used for selection of days considered were collected from the Malaysian meteorological department (MMD, 2014). The rural sites (Fig. 7b) designated "Rural" are situated 2–4 km South of Putrajaya at an elevation (Table 1 and Fig. 1). The prevailing land cover conditions of the rural LCZs are characterized by sparsely built type with low and dense trees source area (Table 1; Figs. 1b and 7b).

Fig. 8 shows mean heating of the area for the selected days with a profile representing the diurnal behaviour of UHI as exhibited in different studies in other cities (Childs & Raman, 2005; Giannaros et al., 2013; Lin et al., 2008). Timing of sunrise and sunset (roughly

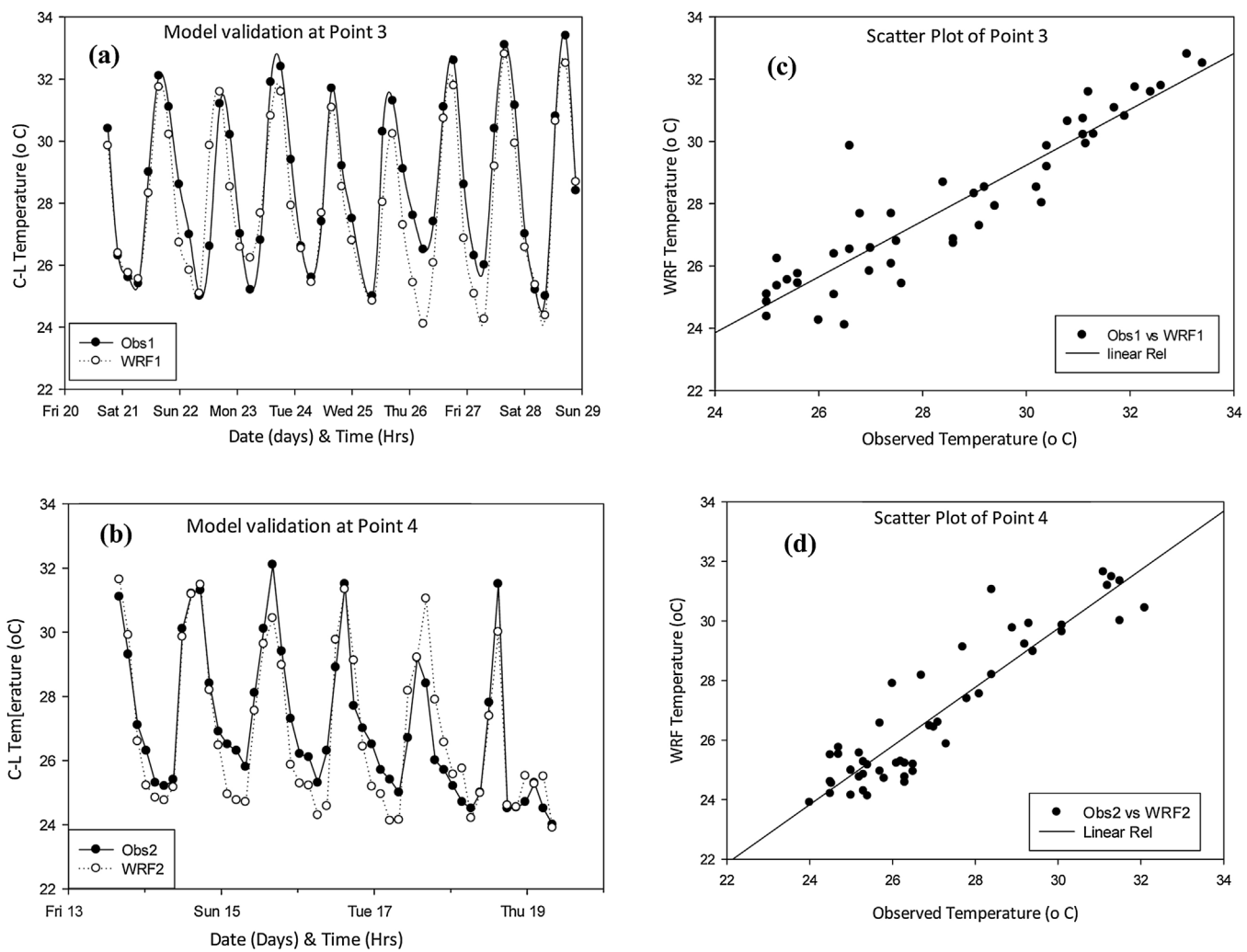


Fig. 4. (a) and (b) Model validation for location P3 and P4 respectively, (c) and (d) are scatter plots for C-L temperatures for location P3 and P4 respectively. WRF1 & 2 indicate model results, while Obs1 & 2 indicate observed results.

0700 and 1900 MST respectively) seems to have induced influence on the magnitude of UHI experienced in the area. During mid-day, intensity of solar energy reaching the surface of the earth in any given local climate is uniform. This has a normalizing induced effects on heating observed in both engineered and semi/natural

surfaces that characterized Putrajaya and the rural sites. Thus negligible urban C-L heating was noticed during mid-hours (1100–1400 MST) of the considered days. However, an urban heat sink was observed between 1300 and 1500 MST.

The term UHI is often associated with rural–urban temperature contrast; however, within an urban area, temperature difference could be noticed between different local climate zones (Fig. 9(b and c)). This is due to the varying factors (such as land cover type, building height, aspect ratio, etc.) that differentiate LCZs. This difference in urban C-L temperature is induced by varying land cover and built type (Figs. 7 and 9). The magnitude of LCZ–LCZ UHI is driven temporally by solar radiation variations. To evaluate the LCZ–LCZ UHI of the area, LCZs with varying built and land cover source area types were selected. Precincts identified as mostly urbanized and highly vegetated were classed into two different groups. Four of the 19 precincts (P12, 13, 19 and 20) were classed “highly vegetated” while the remaining 15 were classed urbanized. Average 24 h C-L temperatures of the highly vegetated precincts were subtracted from the urbanized precincts to yield LCZ UHI profile of Fig. 8c, with a mean LCZ UHI of 0.25 °C (Table 3) for the selected days.

Precinct 8 (Fig. 7e), 3 (Fig. 7f) and 20 (Fig. 7d), described by compact low-rise and paved surface, open midrise and paved surface, and sparsely built and low plants respectively (Table 1) were compared with Precinct 13 (sparsely built and low plants). 13th, 15th,

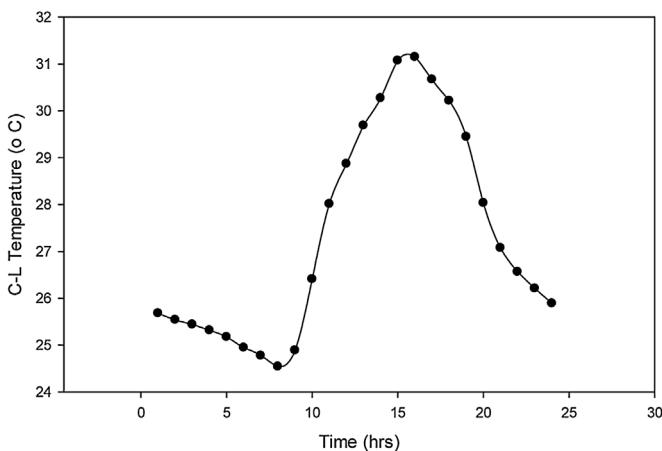


Fig. 5. 24 h average modelled C-L temperature (°C) for the study period – 13/07/2012 to 28/07/2012.

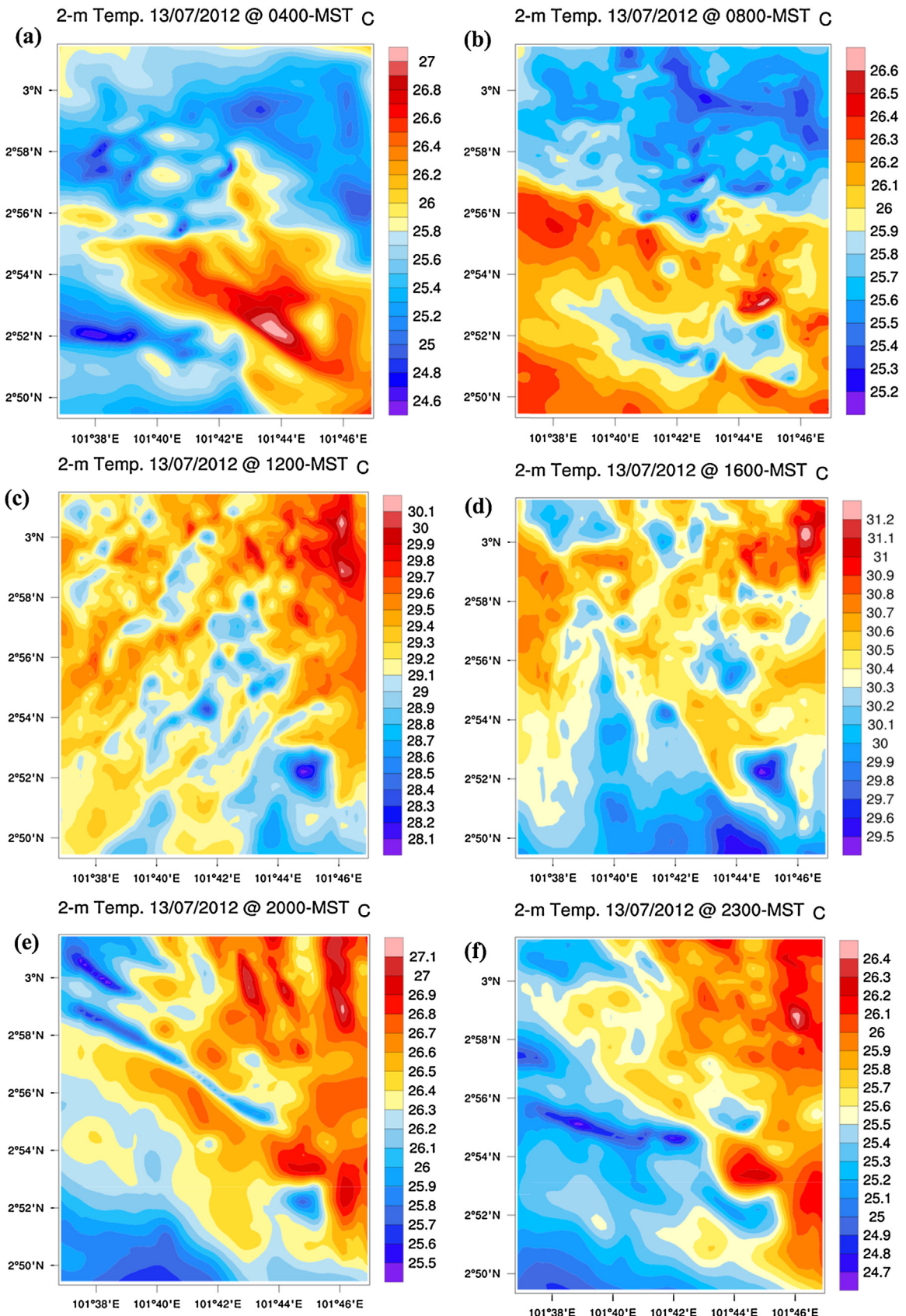


Fig. 6. Modelled spatial and temporal distribution of canopy-layer (2-m) air temperature for 13/07/2012. (a) early morning at 0400 MST, (b) morning at 0800 MST, (c) noon at 1200 MST, (d) daytime at 1600 MST, (e) night at 2000 MST and (f) late night at 2300 MST.

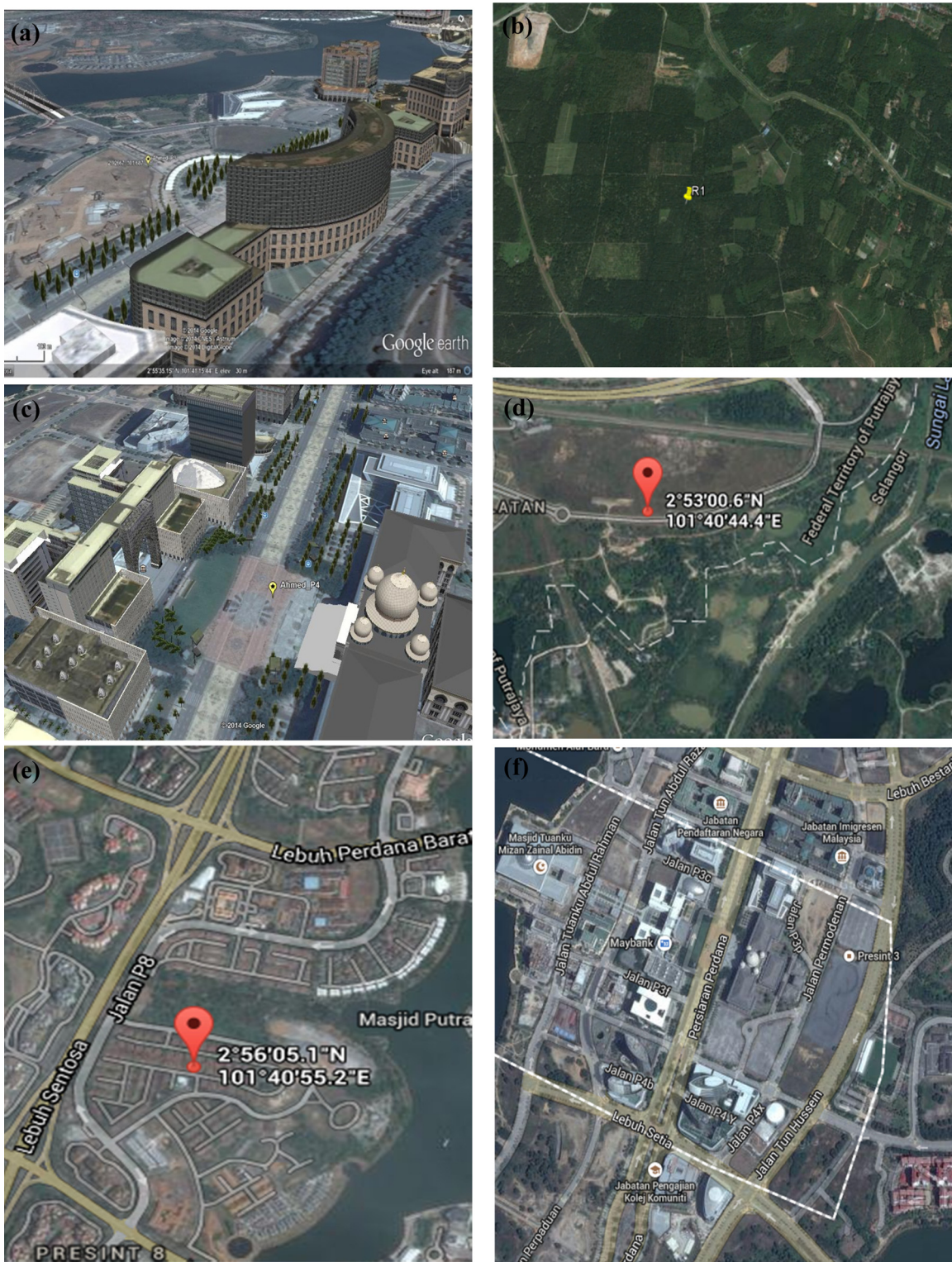


Fig. 7. Google-Earth and Google-map images of the considered areas for this study. (a) site for P3, (b) rural site for UHI study, (c) site for P4, (d) precinct 13, (e) precinct 8 and (f) precinct 3.

18th, 23rd and 26th of July, 2012 were selected to study the UHI phenomenon in the LCZs. Figs. 6 and 9 present the behaviour of the LCL-LCZ UHI and the dependency of its magnitude on built and source area land cover type (Fig. 1b, Table 1 and Fig. 9(a and c)). Open midrise has the highest magnitude and a negligible heating of Precinct 20 was observed.

4.3. Impact of surface materials on UHI intensity

Putrajaya is composed of different LCZs with varying land surface materials (Table 1). These materials have different thermal properties and thus different rate of heat capacity. Fig. 9 portrays the impact of surface materials on the magnitude of UHI. Though

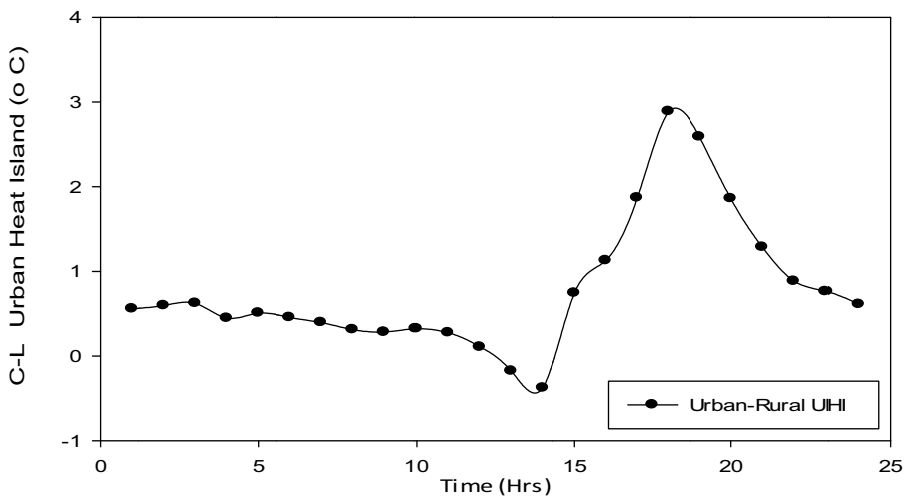


Fig. 8. Average C-L UHI of study sites (Table 1) during 13th, 15th, 18th, 23rd, and 26th of July, 2012.

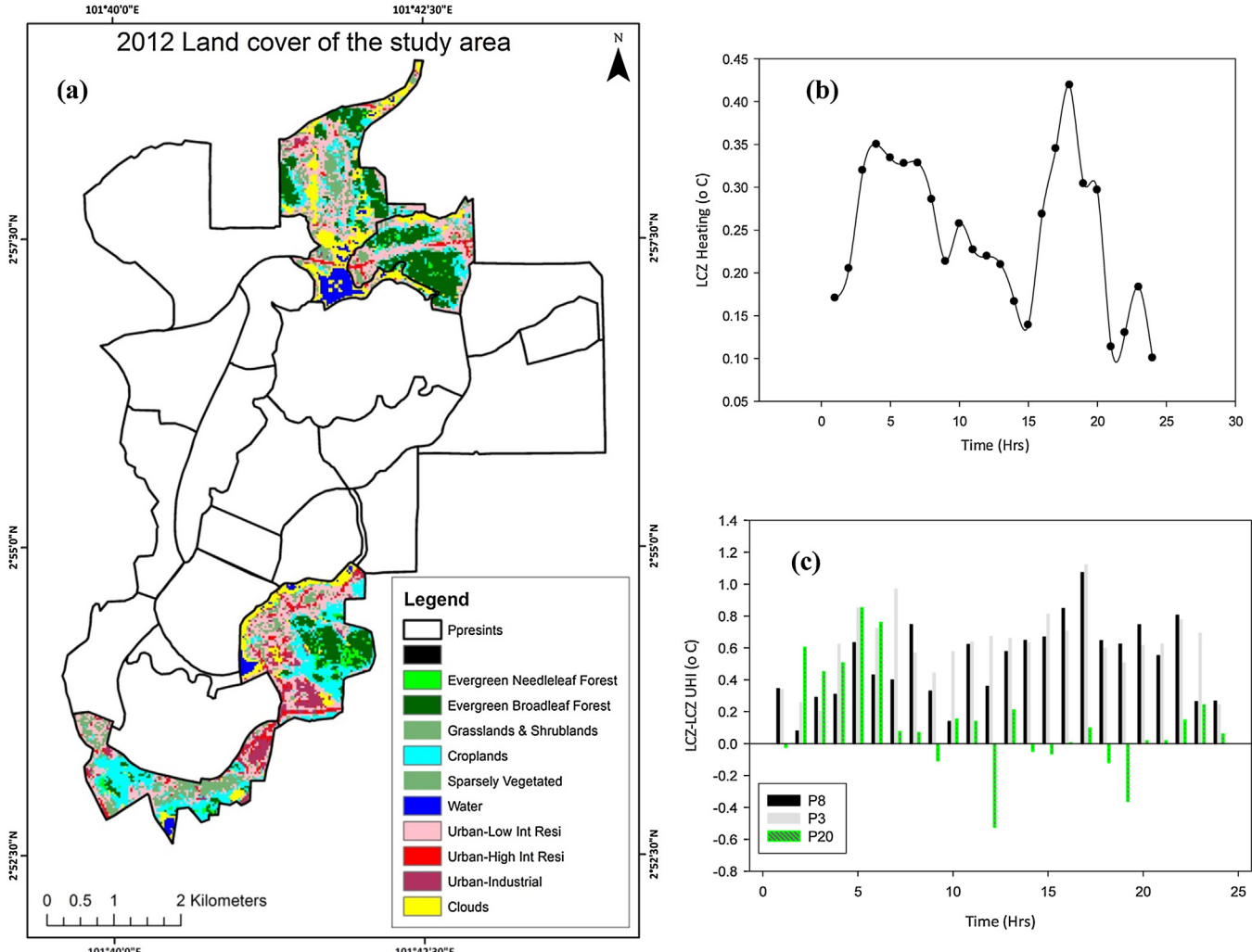


Fig. 9. Differential heating of the studied LCZs in Putrajaya, during 13/07/2012–26/07/2012 (a) Map showing highly vegetated precincts of Putrajaya. (b) Average 24 h UHI between urbanized and highly vegetated precincts. (c) Black, grey and green colour bars representing precinct 8, 3 and 20 respectively.

the number of sites used in this study is too small to generalize on its impact, it is an indication of a plausible contribution and would be further investigated in the next sequel of this study.

4.4. Discussion

The performance of the WRF-model was assessed with data retrieved from ASMA meteorological station and two other in situ measurement sites. Fig. 3a presents the observed and modelled C-L temperatures for the ASMA site designated CAC053. Overall the model performed relatively well for this site and was able to replicate the phase of diurnal cycle with a correlation coefficient of R^2 of 0.81, MAE of 1.69°C , and RSME of 2.03°C (Fig. 4b and Table 2). However, the model overestimated the amplitude of the observed data, especially the night-time minimum temperature. This could imply either the upward heat fluxes or the outgoing long-wave radiation of the area is overestimated. Also, radiation of solar trapping and fluxes from walls and roads, producing high ambient temperatures, inside the urban street as calculated in the UCM may have resulted in this discrepancy since the station is located a few metres radius away from buildings; as such, it is less thermally loaded. The actual causes of the overestimation of temperatures can only be speculated at this stage but could not be concluded due to lack of comprehensive measurements of surface energy balance parameters of the area during the considered period.

Twenty-four hour C-L air temperature average during the study period (13/07/2012 to 28/07/2012), reveals a common trend of diurnal profile of temperature with a minimum and maximum value of 24.5°C and 31.2°C respectively. Temperature increases during the day and decreases at night with minimum and maximum temperature occurring at 0800 and 1600 MST respectively. This is due to variation in the amount of solar radiation exposure during the night and day time. The emergence of sunrise (0700 MST) in the area gradually increases the C-L air temperature from 0800 MST to a peak value between 1400 and 1600 MST. This increase is due to the increasing amount of solar energy reaching the earth's surface. Similarly, after sunset (1900 MST), the amount of solar energy reduces thereby causing the observed decrease in the C-L air temperature (Fig. 5).

The modelled UHII of the rural–urban C-Ls is shown in Fig. 8 for a 5 day average over a 24 h time interval. The UHI was computed by subtracting the C-L air temperature of the rural LCZ sites (R1–R5) from the spatially average urban LCZ sites (Fig. 1b and Table 1). Results reveal the UHI effect is more obvious during night time (1700–2300 MST) than during the day, with a gradual decline in the early morning hours (0100–0600 MST). However, a heat sink was noticed during the hours of 1300–1500 MST. Heat sink is the event of a reverse phenomenon of the UHI (i.e. rural areas having higher temperature contrast than the urban). The urban heat sink formation during the day is encouraged by the accumulative effect of the 37% total land area of Putrajaya reserved for vegetation. Similarly the reserved vegetation has immense impact in normalizing the overall effect of the urbanized LCZs on the urban heat island of the area, despite differential spatial and temporal heating of the precincts. For instance, some areas such as precinct 3, 7, 8 and 9 had a maximum UHII ranging from 1.9 to 3.1°C during the study period.

Furthermore, the increase in the urban heat island intensity during the night is due to the slow nocturnal cooling of the urban LCZs owing to the engineered surfaces used in constructions and building of roads. Horizontal transport would be more pronounced in the rural site due to the prevailing LCZ built type (sparsely built); meaning fewer obstructions to impede advection of re-radiated heat fluxes in the rural sites as opposed to the urban climate zones. A maximum UHII of 3.1°C was observed in Precinct 8 on the 23rd July 2012. However, due to the normalizing effects induced by large

Table 3
Summary of UHI of Putrajaya.

| UHIs | Mean ($^\circ\text{C}$) | Minimum ($^\circ\text{C}$) | Maximum ($^\circ\text{C}$) |
|---|---------------------------|------------------------------|------------------------------|
| Rural–urban UHI | 0.79 | -0.38 | 2.9 |
| UHI between purbanized and vegetated recincts | 0.25 | 0.1 | 0.42 |

amount of vegetation in some of the LCZs within the study area, mean and maximum daily UHII of 0.79 and 2.9°C were respectively observed (Fig. 8 and Table 3).

In an attempt to understand the dynamics of local/micro climates within Putrajaya urban area, comparison between urbanized and highly vegetated precincts has prompted some curiosity in the results observed (Fig. 9b). Variations in heating seem to indicate a trend similar to other class of different local climate heating, but with a non-uniform profile. 0.25°C and 0.42°C mean and maximum 2-m temperature difference between urbanized and highly vegetated precincts were respectively recorded during the study.

Little has been done to understand the temperature difference between LCZs for UHI, especially in tropical areas of Malaysia. To further explore the temperature contrast between LCZs, three different LCZs with distinct built and source area land cover types were selected for this investigation (Fig. 9) on 13th of July, 2012. Fig. 9 presents the temporal observations of the UHII. Precinct 3 with open midrise built type and paved surfaces as source area land cover has the maximum mean UHII with a magnitude of 0.65°C followed by Precinct 8 (Fig. 9 and Table 2), while Precinct 20 has a negligible magnitude of UHI. It is noteworthy that Precinct 20 has same characteristics built type and source area land cover type as Precinct 13. This agrees with Stewart and Oke (2009, 2011) on the impact of land cover and surface properties as the real drivers of local climate difference. Furthermore, Precinct 20 located southward boundary of Putrajaya and Cyberjaya (Fig. 1b and Fig. 9a) is surrounded by highly vegetated areas which could have influenced the reduced heating observed in the precinct by advection. This reduced heating induced repeated heat sink noted in Fig. 9c for precinct 20 at different intervals.

Spatial and temporal patterns of UHII were observed in Fig. 6. Fig. 6 shows the modelled C-L (2-m) air temperatures in the early morning (0400 MST), morning (0800 MST), and noon (1200 MST), during the solar peak time (1600 MST), evening (2000 MST) and late evening (2300 MST). During early morning and night hours, the magnitude of the UHI effect is more pronounced ($>1.5^\circ\text{C}$) while the day time magnitude is negligible where the contour spread is near uniform (Fig. 5e and f). The near-uniform contours contrast starts disappearing as evening approaches (increasing UHII) and then a clear distinction between the contours; which represents spatial difference in temperatures. This agrees with the stated theory of UHI formation (Oke, 1982).

Fig. 9 again highlights the impact of surface materials on the magnitude of UHI. Precinct 8 and 3 are characterized with prevailing paved surfaces. Conversely, Precinct 13 and 20 possess predominantly dense trees and low plants respectively. To further understand the induced influence of surface materials on the area, the average hourly C-L air temperatures of precinct 13 for the computed days were subtracted from the other precincts (3, 8 and 20). Results depict Precincts 3 and 8 having significant UHII as compared to Precinct 20 which shared almost same surface and built type properties. This is as a result of the differences in the albedo of the surfaces (Stewart & Oke, 2012). Greenery is known for their ability to cool the surrounding by evapotranspiration (Rosenfeld et al., 1998; Taha, 1997) and is likely to have induce the low temperature values experienced in the area.

UHI of the city during this study could not be compared with the data obtained by Ahmed et al. (2014) since this study considered its

overall effect on the city whereas Ahmed et al. (2014) was focused on the Putrajaya main boulevard. UHI studies conducted in Kuala Lumpur (Ahmad et al., 2010; Ahmed et al., 2014; Ahmad & Hashim, 2007; Elsayed, 2012a) shows that the UHII observed in Putrajaya is relatively low and this could be accounted for by the 37% of the total land area reserved for vegetation and the yet to be developed areas bid to be completed in 2025. It is evident that the garden city concept adopted for the design and development of the city made some positive impact on the magnitude of UHI observed during this study period.

5. Conclusions

In this study the single-layer urban canopy model was coupled with the WRF/Noah LSM modelling system over Putrajaya to investigate the UHI and performance of the garden-city concept adopted during the development of the area. Meteorological data from ASMA and in situ data from Ahmed et al. (2014) were used for the validations of the model.

Comparison of the model results with data used for validations shows reasonable correlation and performance. The model was able to capture the phase cycle and diurnal behaviour of the validated data, and successfully simulated some of the features of UHI effects such as day and night variations in magnitude. Hence, the model has displayed suitability for use in the study of UHI phenomenon, spatial and temporal variations of temperature in the area.

UHI intensity of Putrajaya varies temporally and spatially, with a maximum magnitude of 3.1 °C observed on 23rd July 2012. However, daily 0.79 °C and 2.9 °C mean and maximum rural–urban heat island intensity were observed in Putrajaya over the study period. A preliminary comparison of different LCZs shows influences of land cover type on the magnitude of UHI. Furthermore, UHII during the night ranges from 1.9 to 3.1 °C. The reserved total land area for vegetation had influence on the overall magnitude of the UHII in Putrajaya. Spatial and temporal variation of C-L temperature and UHII was also noticed in this study with LCZ–LCZ UHI of the study area was also successfully investigated. Furthermore, a daily average LCZ UHII of 0.25 °C between urbanized and highly vegetated precincts was obtained.

The results from the study indicate less heating of the area compared to other cities; nevertheless, there is still need to further reduce the C-L air temperature of the area in order to achieve the modern garden city plan and the country's pledge to adhere to environmental standards. These preliminary findings would help in optimizing the WRF models and facilitate more improvement on the numerical measurement of air temperature and UHI phenomenon in the area.

Acknowledgements

This current study is conducted with support through the e-Science fund of the Ministry of Science, Technology and Innovation (MOSTI) with contract number M0056.54.01. The authors would also like to thank Adeeb Qaid Ahmed for supplying the data used for validation of the numerical model employed in this study. Also, we are grateful for access to the University of Nottingham High Performance Computing Facility for part of the numerical calculations.

References

- Aekbal, S., Abd, Z., Mohd, W., & Wan, N. (2013). Social and factors contributing to the formation of an urban heat island in Putrajaya, Malaysia. In *Procedia – Social and Behavioural Sciences*, 00(UE–004), 1–11 <http://dx.doi.org/10.1016/j.sbspro.2013.11.086>
- Aguilar, E., Auer, I., Brunet, M., Peterson, T. C., & Wieringa, J. (2003). In P. Llansó (Ed.), *Guidelines on climate metadata and homogenization*. WMO Tech Doc. 1186. Geneva: World Meteorological Organization.
- Ahmad, S., & Hashim, N. (2007). Effects of soil moisture on urban heat island occurrences: Case of Selangor, Malaysia. *Humanity & Social Sciences Journal*, 2(2), 132–138.
- Ahmad, S., Hashim, N., & Jani, Y. M. (2009). Fenomena Pulau Haba Bandar dan isu alam sekitar di Bandaraya Kuala Lumpur The Urban Heat Island phenomenon and the environmental issues of Kuala Lumpur city. *Malaysian Journal of Society and Space*, 5(3), 57–67. Retrieved from <http://www.ukm.edu.my/geografi/images/upload/5/2009-3-shahruddin-melayu.pdf>
- Ahmad, S., Hashim, N., Jani, Y. M., Aiyub, K., & Mahmud, M. F. (2010). The effects of different land uses on the temperature distribution in urban areas. In *SEAGA 2010-Online Proceedings Hanoi*, (pp. 1–18). Retrieved from <http://seaga.xtreemhost.com/seaga2010/CS4B-Shah.pdf>
- Ahmed, A. Q., Ossen, D. R., Jamei, E., Manaf, N. A., Said, I., & Ahmad, M. H. (2014). Urban surface temperature behaviour and heat island effect in a tropical planned city. *Theoretical and Applied Climatology*, <http://dx.doi.org/10.1007/s00704-014-1122-2>
- Akbari, H. (2005). Energy saving potentials and air quality benefits of urban heat island mitigation. In *First International Conference on Passive and Low Energy Cooling for the Built Environment* Athens, Greece, (pp. 1–19), doi:DE-AC02-05CH11231.
- Alsharif, A. A. A., & Pradhan, B. (2013). Urban sprawl analysis of Tripoli metropolitan city (Libya) using remote sensing data and multivariate logistic regression model. *Journal of the Indian Society of Remote Sensing*, 42(1), 149–163. <http://dx.doi.org/10.1007/s12524-013-0299-7>
- Barker, T. (2007). Climate change 2007: An assessment of the intergovernmental panel on climate change. In R. K. Pachauri, & A. Reisinger (Eds.), *Change* (Vol. 446). Valencia, Spain: IPCC. <http://dx.doi.org/10.1256/004316502320517344>
- Bigon, L. (2012). Garden city in the tropics? French Dakar in comparative perspective. *Journal of Historical Geography*, 38(1), 35–44. <http://dx.doi.org/10.1016/j.jhg.2011.07.005>
- Bunnell, T. (2002). Multimedia utopia? A geographical critique of high-tech development in Malaysia's multimedia super corridor. *Antipode*, 34(2), 265–295. <http://dx.doi.org/10.1111/1467-8330.00238>
- Chen, F., & Dudhia, J. (2001). Coupling an advanced land surface – hydrology model with the Penn state – NCAR MM5 modeling system. Part I. Model implementation and sensitivity. *Monthly Weather Review*, 129(4), 569–585. [http://dx.doi.org/10.1175/1520-0493\(2001\)129<0569:CAALSH>2.0.CO;2](http://dx.doi.org/10.1175/1520-0493(2001)129<0569:CAALSH>2.0.CO;2)
- Childs, P. P., & Raman, S. (2005). Observations and numerical simulations of urban heat island and sea breeze circulations over New York City. *Pure and Applied Geophysics*, 162(10), 1955–1980. <http://dx.doi.org/10.1007/s00024-005-2700-0>
- Chin, H. S. (2006). Putrajaya – administrative centre of Malaysia – planning concept and implementation. In *Sustainable urban development and Governance conference at Sungkyunkwan University Seoul Seoul*, Korea, (pp. 1–20). Retrieved from http://eprints.utm.my/6622/1/HoChinSiong2006_Putrajaya-AdministrativeCentreOfMalaysia.pdf
- Chou, S. (2011). An example of vertical resolution impact on WRF-Var analysis. *Electronic Journal of Operational Meteorology*, (May), EJ05. Retrieved from <http://www.nwas.org/ej/pdf/2011-EJ5.pdf>
- DOE. (2013). *Hourly surface observational data*.
- Dudhia, J. (1989). Numerical study of convection observed during the winter monsoon experiment using a mesoscale two-dimensional model. *Journal of the Atmospheric Sciences*, 46(20), 3077–3107. [http://dx.doi.org/10.1175/1520-0469\(1989\)046%253C3077:NSOCOD%253E2.0.CO;2](http://dx.doi.org/10.1175/1520-0469(1989)046%253C3077:NSOCOD%253E2.0.CO;2)
- Dudhia, J., Hong, S.-Y., & Lim, K.-S. (2008). A new method for representing mixed-phase particle fall speeds in bulk microphysics parameterizations. *Journal of the Meteorological Society of Japan*, 86A, 33–44. <http://dx.doi.org/10.2151/jmsj.86A.33>
- Elsayed, I. S. M. (2011). A study on the urban heat island of the city of Kuala Lumpur, Malaysia. In *19th Conference on Applied Climatology* (pp. 1–6). Asheville, NC: American Meteorological Society.
- Elsayed, I. S. M. (2012). Mitigation of the urban heat island of the city of Kuala Lumpur, Malaysia. *Middle-East Journal of Scientific Research*, 11(11), 1602–1613. <http://dx.doi.org/10.5829/idosi.mejsr.2012.11.11.1590>
- Elsayed, I. (2012a). *Effects of urbanization on the urban heat island of Kuala Lumpur city*. Saarbrücken, Germany: LAP LAMBERT Academic Publishing. Retrieved from <https://www.lap-publishing.com/catalog/details//store/gb/book/978-3-8484-8039-5/effects-of-urbanization-on-the-urban-heat-island-of-kuala-lumpur-city>
- Elsayed, I. (2012b). *Effects of urbanization on the urban heat island of Kuala Lumpur city: UHI as a global issue Kl & urbanization research method data & findings analysis & synthesis conclusion*. LAP LAMBERT Academic Publishing.
- Enete, I. C., Officha, M., & Ogbonna, C. E. (2012). Urban heat island magnitude and discomfort in Enugu urban area, Nigeria. *Journal of Environment and Earth Science*, 2(7), 77–83. Retrieved from <http://www.iiste.org/Journals/index.php/JEES/article/view/2522>
- Feng, J.-M., Wang, Y.-L., Ma, Z.-G., & Liu, Y.-H. (2012). Simulating the regional impacts of urbanization and anthropogenic heat release on climate across China. *Journal of Climate*, 25(20), 7187–7203. <http://dx.doi.org/10.1175/JCLI-D-11-00333.1>
- Fire and Disaster Management Agency of Japan (2011).
- Giannaros, T. M., Melas, D., Daglis, I. A., Keramitsoglou, I., & Kourtidis, K. (2013). Numerical study of the urban heat island over Athens (Greece) with the WRF model. *Atmospheric Environment*, 73(0), 103–111. <http://dx.doi.org/10.1016/j.atmosenv.2013.02.055>
- Hien, W. N., & Jusuf, S. K. (2010). Air temperature distribution and the influence of sky view factor in a green Singapore estate. *Journal of Urban Planning and*

- Development*, 136(3), 261–272. [http://dx.doi.org/10.1061/\(ASCE\)UP.1943-5444.000014](http://dx.doi.org/10.1061/(ASCE)UP.1943-5444.000014)
- Hirano, Y., & Fujita, T. (2012). Evaluation of the impact of the urban heat island on residential and commercial energy consumption in Tokyo. *Energy*, 37(1), 371–383. <http://dx.doi.org/10.1016/j.energy.2011.11.018>
- Hong, S.-Y., Ji, D., & Chen, S.-H. (2004). A revised approach to ice microphysical processes for the bulk parameterization of clouds and precipitation. *Monthly Weather Review*, 132(1), 103–120. [http://dx.doi.org/10.1175/1520-0493\(2004\)132<0103:ARATIM>2.0.CO;2](http://dx.doi.org/10.1175/1520-0493(2004)132<0103:ARATIM>2.0.CO;2)
- Hong, S.-Y., Noh, Y., & Dudhia, J. (2006). A new vertical diffusion package with an explicit treatment of *Monthly Weather Review*, 134(9), 2318–2341. <http://dx.doi.org/10.1175/MWR3199.1>
- Howard, E. (1946). Garden cities of to-morrow. In F. J. Osborn (Ed.), *An introductory essay by Lewis Mumford*. London: Faber and Faber, pp. 50–57, 138–147. Retrieved from <http://urbanplanning.library.cornell.edu/DOCS/howard.htm>
- Hu, Z., Yu, B., Chen, Z., Li, T., & Liu, M. (2012). Numerical investigation on the urban heat island in an entire city with an urban porous media model. *Atmospheric Environment*, 47(0), 509–518. <http://dx.doi.org/10.1016/j.atmosenv.2011.09.064>
- Ibrahim, I., & Samah, A. A. (2011). Preliminary study of urban heat island: Measurement of ambient temperature and relative humidity in relation to landcover in Kuala Lumpur. In *2011 19th International Conference on Geoinformatics* (pp. 1–5). Shanghai: IEEE. <http://dx.doi.org/10.1109/GeoInformatics.2011.5981068>
- Ihara, T., Kusaka, H., Hara, M., Matsuhashi, R., & Yoshida, Y. (2011). Estimation of mild health disorder caused by urban air temperature increase with midpoint-type impact assessment methodology. *Journal of Environmental Engineering*, 76, 459–467.
- Inostroza, L., Baur, R., & Csaplovics, E. (2013). Urban sprawl and fragmentation in Latin America: A dynamic quantification and characterization of spatial patterns. *Journal of Environmental Management*, 115, 87–97. <http://dx.doi.org/10.1016/j.jenvman.2012.11.007>
- IPCC. (2001). In X. Houghton, J. T. Ding, Y. Griggs, D. J. Noguer, M. van der Linden, P. J. Dai, C. Maskell, & K. Johnson (Eds.), *Climate change 2001: The scientific basis*. United Kingdom and New York, NY, USA: Cambridge University Press, Cambridge.
- Johnson, C. (2008). Green modernism: The irony of the modern garden cities in southeast Asia. In *In 44th ISOCARP Congress Dalian, China*, (pp. 1–11). Retrieved from http://www.isocarp.net/data/case_studies/1364.pdf
- Kain, J. S. (2004). The Kain–Fritsch convective parameterization: An update. *Journal of Applied Meteorology*, 41(1), 170–181. [http://dx.doi.org/10.1175/1520-0450\(2004\)043<0170:TKCPAU>2.0.CO;2](http://dx.doi.org/10.1175/1520-0450(2004)043<0170:TKCPAU>2.0.CO;2)
- Kolokotroni, M., Giannitsaris, I., & Watkins, R. (2006). The effect of the London urban heat island on building summer cooling demand and night ventilation strategies. *Solar Energy*, 80(4), 383–392. <http://dx.doi.org/10.1016/j.solener.2005.03.010>
- Konopacki, S., & Akbari, H. (2002). *Energy savings for heat-island reduction strategies in Chicago and Houston (including updates for Baton Rouge, Sacramento, and Salt Lake City)*. Berkeley., doi:LBNL-49638.
- Laprise, R. (1992). The Euler equations of motion with hydrostatic pressure as an independent variable. *Monthly Weather Review*, 120(1), 197–207. [http://dx.doi.org/10.1175/1520-0493\(1992\)120<0197:TEOMW>2.0.CO;2](http://dx.doi.org/10.1175/1520-0493(1992)120<0197:TEOMW>2.0.CO;2)
- Lin, C.-Y., Chen, F., Huang, J. C., Chen, W.-C., Liou, Y.-A., Chen, W.-N., et al. (2008). Urban heat island effect and its impact on boundary layer development and land-sea circulation over northern Taiwan. *Atmospheric Environment*, 42(22), 5635–5649. <http://dx.doi.org/10.1016/j.atmosenv.2008.03.015>
- Macedo, J. (2011). Maringá: A British garden city in the tropics. *Cities*, 28(4), 347–359. <http://dx.doi.org/10.1016/j.cities.2010.11.003>
- Marrapu, P. (2012). *Local and regional interactions between air quality and climate in New Delhi: A sector based analysis*. University of Iowa.
- Martilli, A. (2014). An idealized study of city structure, urban climate, energy consumption, and air quality. *Urban Climate*, 1–17. <http://dx.doi.org/10.1016/j.jclim.2014.03.003>
- Md Din, M. F., Lee, Y. Y., Ponraj, M., Ossen, D. R., Iwao, K., & Chelliapan, S. (2014). Thermal comfort of various building layouts with a proposed discomfort index range for tropical climate. *Journal of Thermal Biology*, 41, 6–15. <http://dx.doi.org/10.1016/j.jtherbio.2014.01.004>
- Mercader, J., Codina, B., Sairouni, A., & Cunillera, J. (2010). Results of the meteorological model WRF-ARW over Catalonia, using different parameterizations of convection and cloud microphysics. *Tethys, Journal of Weather and Climate of the Western Mediterranean*, 75–86. <http://dx.doi.org/10.3369/tethys.2010.0707>
- Miao, S., Chen, F., LeMone, M. A., Tewari, M., Li, Q., & Wang, Y. (2009). An observational and modeling study of characteristics of urban heat island and boundary layer structures in Beijing. *Journal of Applied Meteorology and Climatology*, 48(3), 484–501. <http://dx.doi.org/10.1175/2008JAMC1909.1>
- Middel a Brazel, A., Kaplan, S., & Myint, S. (2012). Daytime cooling efficiency and diurnal energy balance in Phoenix, Arizona, USA. *Climate Research*, 54(1), 21–34. <http://dx.doi.org/10.3354/cr01103>
- Mlawer, E. J., Taubman, J., Brown, P. D., Iacono, M. J., & Clough, S. A. (1997). Radiative transfer for inhomogeneous atmospheres: RRTM, a validated correlatedk model for the longwave. *Journal of Geophysical Research*, 102(D14), 16663–16682. <http://dx.doi.org/10.1029/97JD00237>
- MMD. (2014). *Malaysian meteorological department*. Retrieved from www.met.gov.my
- Moser, S. (2010). Putrajaya: Malaysia's new federal administrative capital. *Cities*, 27(4), 285–297.
- NCAR. (2014). *Terrestrial input data*. Retrieved from http://www2.mmm.ucar.edu/wrf/OnLineTutorial/Basics/GEOGRID/ter_data.htm
- NCEP. (2000). *National Centers for Environmental Prediction/National Weather Service/NOAA/U.S. Department of Commerce*. 2000. Updated daily. , doi: 10.5065/D6M043C6.
- Offerle, B., Grimmond, C. S. B., & Fortuniak, K. (2005). Heat storage and anthropogenic heat flux in relation to the energy balance of a central European city centre. *International Journal of Climatology*, 25(10), 1405–1419. <http://dx.doi.org/10.1002/joc.1198>
- Oke, T. R. (1982). The energetic basis of the urban heat island. *Quarterly Journal of the Royal Meteorological Society*, 108(455), 1–24. <http://dx.doi.org/10.1002/qj.49710845502>
- Oke, T. R. (1988a). *Boundary layer climates* (2nd ed.). Routledge.
- Oke, T. R. (1988b). Street design and urban canopy layer climate. *Energy and Buildings*, 11(1–3), 103–113. [http://dx.doi.org/10.1016/0378-7788\(88\)90026-6](http://dx.doi.org/10.1016/0378-7788(88)90026-6)
- Oke, T. R. (2004). *Initial guidance to obtain representative meteorological observations at urban sites*. IOM Rep. 81, WMO. Tech. Doc. No. 1250. Geneva: World Meteorological Organization. Retrieved from <http://www.wmo.int/pages/prog/www/IMOP/publications/IOM-81/IOM-81-UrbanMetObs.pdf>
- Qiao, Z., Tian, G., & Xiao, L. (2013). Diurnal and seasonal impacts of urbanization on the urban thermal environment: A case study of Beijing using MODIS data. *ISPRS Journal of Photogrammetry and Remote Sensing*, 85, 93–101. <http://dx.doi.org/10.1016/j.isprsjprs.2013.08.010>
- Rosenfeld, A. H., Akbari, H., Romm, J. J., & Pomerantz, M. (1998). Cool communities: Strategies for heat island mitigation and smog reduction. *Energy and Buildings*, 28(1), 51–62. [http://dx.doi.org/10.1016/S0378-7788\(97\)00063-7](http://dx.doi.org/10.1016/S0378-7788(97)00063-7)
- Sailor, D. J., & Lu, L. (2004). A top-down methodology for developing diurnal and seasonal anthropogenic heating profiles for urban areas. *Atmospheric Environment*, 38(17), 2737–2748. <http://dx.doi.org/10.1016/j.atmosenv.2004.01.034>
- Sani, S. (1984). Urban development and changing patterns of night time temperatures in the Kuala Lumpur-Petaling Jaya Area Malaysia. *Jurnal Teknologi*, 5(1) <http://dx.doi.org/10.11113/jt.v5.937>
- Shaharuddin, A., Noorazuan, M., Yaakob, M., & Noraziah, A. (2011). Accelerated urbanisation and the changing trend of rainfall in tropical urban areas. *World Applied Sciences Journal*, 13, 69–73.
- Shahidan, M. F., Jones, P. J., Gwilliam, J., & Salleh, E. (2012). An evaluation of outdoor and building environment cooling achieved through combination modification of trees with ground materials. *Building and Environment*, 58, 245–257. <http://dx.doi.org/10.1016/j.buildenv.2012.07.012>
- Shem, W., & Shepherd, M. (2009). On the impact of urbanization on summer-time thunderstorms in Atlanta: Two numerical model case studies. *Atmospheric Research*, 92(2), 172–189. <http://dx.doi.org/10.1016/j.atmosres.2008.09.013>
- Skamarock, W. C., Klemp, J. B., Dudhia, J., Gill, D. O., Barker, D. M., Duda, M. G., et al. (2008). *A description of the advanced research WRF version 3. NCAR technical note*. Boulder, CO, USA: National Center for Atmospheric Research: Mesoscale and Microscale Meteorology Division. Retrieved from http://www2.mmm.ucar.edu/wrf/users/docs/arw_v3.pdf
- Stewart, I. D. (2011). A systematic review and scientific critique of methodology in modern urban heat island literature. *International Journal of Climatology*, 31(2), 200–217. <http://dx.doi.org/10.1002/joc.2141>
- Stewart, I., & Oke, T. (2009). Classifying urban climate field sites by local climate zones: The case of Nagano, Japan. In *The seventh International Conference on Urban Climate Yokohama*, Japan, (pp. 1–5).
- Stewart, I., & Oke, T. (2011). Local climate zones: Application to heat island studies in tropical regions. In *Workshop on urban climatology in tropical and sub-tropical regions*. Hong Kong: The Chinese University of Hong Kong. Retrieved from <http://iainstew.files.wordpress.com/2013/01/hong-kong-2011.pdf>
- Stewart, I. D., & Oke, T. R. (2012). Local climate zones for urban temperature studies. *Bulletin of the American Meteorological Society*, 93(12), 1879–1900. <http://dx.doi.org/10.1175/BAMS-D-11-00019.1>
- Stewart, I. D., Oke, T. R., & Krayenhoff, E. S. (2014). Evaluation of the local climate zone scheme using temperature observations and model simulations. *International Journal of Climatology*, 34(4), 1062–1080. <http://dx.doi.org/10.1002/joc.3746>
- Subramania Pillai, S., & Yoshie, R. (2012). Experimental and numerical studies on convective heat transfer from various urban canopy configurations. *Journal of Wind Engineering and Industrial Aerodynamics*, 104–106, 447–454. <http://dx.doi.org/10.1016/j.jweia.2012.03.010>
- Taha, H. (1997). Urban climates and heat islands: Albedo, evapotranspiration, and anthropogenic heat. *Energy and Buildings*, 25(2), 99–103. [http://dx.doi.org/10.1016/S0378-7788\(96\)00999-1](http://dx.doi.org/10.1016/S0378-7788(96)00999-1)
- Tran, H., Uchihama, D., Ochi, S., & Yasuoka, Y. (2006). Assessment with satellite data of the urban heat island effects in Asian mega cities. *International Journal of Applied Earth Observation and Geoinformation*, 8(1), 34–48. <http://dx.doi.org/10.1016/j.jag.2005.05.003>
- Uejio, C. K., Wilhelmi, O. V., Golden, J. S., Mills, D. M., Gulino, S. P., & Samenow, J. P. (2011). Intra-urban societal vulnerability to extreme heat: The role of heat exposure and the built environment, socioeconomics, and neighborhood stability. *Health & Place*, 17(2), 498–507. <http://dx.doi.org/10.1016/j.healthplace.2010.12.005>
- Van Weverberg, K., De Ridder, K., & Van Rompaey, A. (2008). Modeling the contribution of the Brussels heat island to a long temperature time series. *Journal of Applied Meteorology and Climatology*, 47(4), 976–990. <http://dx.doi.org/10.1175/2007JAMC1482.1>
- Wang, T., Jiang, F., Deng, J., Shen, Y., Fu, Q., Wang, Q., et al. (2012). Urban air quality and regional haze weather forecast for Yangtze River Delta region. *Atmospheric Environment*, 58(2), 70–83. <http://dx.doi.org/10.1016/j.atmosenv.2012.01.014>
- Wijeyesekera, D. C., Affida, N., Binti, R., Nazari, M., Lim, S. M., Idrus, M., et al. (2012). Investigation into the urban heat island effects from asphalt

- pavements. *OIDA International Journal of Sustainable Development*, 5(6), 97–118.
- Xin, L. Z., Bo, L., & Li, Z. L. (2011). Water resource's ecological counteraccusation towards garden city. *Procedia Environmental Sciences*, 10(ESIAT), 2518–2524. <http://dx.doi.org/10.1016/j.proenv.2011.09.392>
- Yang, X. (2013). *Temporal variation of urban surface and air temperature*. University of Hong Kong. Retrieved from <http://hub.hku.hk/handle/10722/195964>
- Yusof, M., & Johari, M. (2012). Identifying green spaces in Kuala Lumpur using. *Alam Cipta*, 5(2), 93–106. Retrieved from <http://frsb.upm.edu.my/alamcipta/index.php/alamcipta/article/view/30>
- Yusuf, Y. A., Pradhan, B., & Idrees, M. O. (2014). Spatio-temporal assessment of urban heat island effects in Kuala Lumpur metropolitan city using landsat images. *Journal of the Indian Society of Remote Sensing*, <http://dx.doi.org/10.1007/s12524-013-0342-8>
- Zeng, C., Liu, Y., Stein, A., & Jiao, L. (2015). Characterization and spatial modeling of urban sprawl in the Wuhan Metropolitan Area, China. *International Journal of Applied Earth Observation and Geoinformation*, 34, 10–24. <http://dx.doi.org/10.1016/j.jag.2014.06.012>